



Research article

Potential usage of biosynthesized zinc oxide nanoparticles from mangosteen peel ethanol extract to inhibit *Xanthomonas oryzae* and promote rice growth

Titiradsadakorn Jaithon^{a,1}, Thamonwan Atichakaro^{a,1}, Wannarat Phonphoem^a, Jiraroj T-Thienprasert^{b,c}, Tanee Sreewongchai^d, Nattanan Panjaworayan T-Thienprasert^{a,*}

^a Department of Biochemistry, Faculty of Science, Kasetsart University, Bangkok, Thailand

^b Department of Physics, Faculty of Science, Kasetsart University, Bangkok, Thailand

^c Thailand Center of Excellence in Physics, Ministry of Higher Education, Science, Research and Innovation, Bangkok, Thailand

^d Department of Agronomy, Faculty of Agriculture, Kasetsart University, Bangkok, Thailand

ARTICLE INFO

Keywords:

Zinc oxide nanoparticles
Rice
Antibacterial activity
Biosynthesis
Photosynthetic pigment

ABSTRACT

In recent decades, the biosynthesis of nanoparticles using biological agents, such as plant extracts, has grown in popularity due to their environmental and economic benefits. Therefore, this study investigated into utilizing ethanol crude extract sourced from mangosteen peel for the synthesis of zinc oxide nanoparticles (ZnO NPs) and assessing their efficacy against the rice blight pathogen (*Xanthomonas oryzae* pv. *oryzae*) through antibacterial evaluations. Additionally, the effects of the synthesized ZnO NPs on rice plant growth was investigated. The X-ray diffraction analysis revealed the production of wurtzite ZnO NPs under specific synthesis conditions, exhibiting a crystallite size of 38.71 nm (or 387.122 Å) without any contamination. Analysis of the ultraviolet–visible optical absorption spectrum indicated a characteristic absorption peak at 363 nm, suggesting a calculated band gap energy of 2.88 eV for the ZnO NPs. Furthermore, Fourier transform infrared spectroscopy analysis confirmed the presence of active compounds functional groups from mangosteen peel in the synthesized ZnO NPs. These biosynthesized ZnO NPs demonstrated significant inhibition of *X. oryzae* pv. *oryzae* growth, exhibiting an *in vitro* 50 % inhibitory concentration (IC₅₀) value of 1.895 mg/mL and a minimum inhibitory concentration (MIC) value of 4 mg/mL. The ZnO NPs treatments at two-fold IC₅₀ values significantly enhanced root length, dry biomass, and chlorophyll *a* content in rice plants. Consequently, the results demonstrated the potential application of biosynthesized ZnO NPs from mangosteen peel extract in green agriculture, as an alternative to excessive antibiotic use, for combating bacterial plant diseases, and for enhancing plant growth.

* Corresponding author. Department of Biochemistry, Faculty of Science, Kasetsart University, Bangkok, Thailand.

E-mail address: fscinnp@ku.ac.th (N.P. T-Thienprasert).

¹ Co-first authorship.

<https://doi.org/10.1016/j.heliyon.2024.e24076>

Received 2 October 2023; Received in revised form 16 December 2023; Accepted 3 January 2024

Available online 7 January 2024

2405-8440/© 2024 The Authors. Published by Elsevier Ltd. This is an open access article under the CC BY-NC-ND license (<http://creativecommons.org/licenses/by-nc-nd/4.0/>).

1. Introduction

Zinc oxide (ZnO NPs) stands out as one of the extensively employed nanomaterials, finding applications across a diverse range of industrial products such as paints, sunscreens, cosmetics and fabrics, anti-reflection coatings, solar cells, sensors, piezoelectric devices, and in drug delivery [1]. Additionally, ZnO NPs have strong antibacterial properties that can be applied to agriculture [2] and they could increase agricultural productivity under stress conditions [3].

In recent times, the utilization of bio-waste materials for the eco-friendly synthesis of ZnO NPs has garnered significant attention, owing to its feasibility, environmentally friendly, cost effectiveness, and potential to increase waste value [4,5]. According to reports, bio-waste contains a variety of secondary metabolites, such as phenolic acids, alkaloids, flavonoids, and terpenoids [6,7]. These compounds possess the capability to facilitate the generation of ZnO NPs via a redox process, acting as both reducing or capping agents and aiding in the stabilization of ZnO NPs formation [8].

Mangosteen (*Garcinia mangostana* L.) peel extract is rich in phenolic compounds, such as protocatechuic acid [9] and tannins, flavonoids, xanthenes or α -mangostin, and anthocyanins [10]. In Southeast Asia, traditional medicine has utilized mangosteen peel extract to treat skin infections, wounds, diarrhea, and inflammation because mangosteen peel extract has demonstrated antioxidant, antibacterial, and anti-inflammation properties [11]. Lately, the utilization of mangosteen peel extract has extended to the biosynthesis of various nanoparticles, including titanium dioxide [12] and nanoparticles of silver and gold [13].

The primary cause of the blight rice disease is *Xanthomonas oryzae* pv. *oryzae*. It multiplies in the epitheme, then moves and actively multiplies in the xylem, giving symptoms of the blight disease on rice leaves. It spreads through incisions or hydathodes [14]. Various disease management approaches have been used in the past to prevent the disease and reduce yield losses. The application of streptomycin, one of the first discovered aminoglycoside antibiotics, along with other bactericides, remains a crucial method for disease control in many Asian countries. However, the emergence of pathogenic mutants resulting from the use of antibiotics, including streptomycin, poses a significant obstacle [15]. Therefore, alternative techniques are required, such as nanotechnology, to manage this serious disease.

Several reports have demonstrated potential agricultural applications of biosynthesized ZnO NPs. For example, green synthesized ZnO NPs from *Citrus medica* peel extract showed antimicrobial activity against plant pathogenic organisms including *Streptomyces sannanensis*, *Bacillus subtilis*, *Pseudomonas aeruginosa*, *Salmonella enterica*, *Candida albicans* and *Aspergillus niger* [16]. Moreover, the synthesized ZnO NPs could potentially be a nanofertilizer and biosimulant for plants [17]. Using a water extract of mangosteen peel, ZnO NPs were successfully synthesized and demonstrated effective antibacterial properties against plant pathogenic diseases such as *Xanthomonas oryzae* pv. *oryzae*, *Xanthomonas axonopodis* pv. *citri* (causing citrus canker disease), and *Ralstonia solanacearum* (associated with bacterial wilt disease) [18].

Although ethanol extraction was reported as the preferred solvent for extracting antioxidant compounds from mangosteen peel [19], there has been no prior publication on the green synthesis of ZnO NPs using mangosteen peel ethanol extract. Additionally, the choice of solvent is considered a key factor in synthesizing ZnO NPs through a solution-based method, as its polar characteristic significantly impact the nucleation and growth of ZnO NPs, determining their shape and size [20,21]. Therefore, the current study focuses on synthesizing ZnO NPs using mangosteen peel ethanol extract. The physical properties of these ZnO NPs were subsequently investigated using techniques including X-ray diffraction (XRD), ultraviolet-visible (UV-Vis) spectroscopy, scanning electron microscopy (SEM), and Fourier transform infrared (FT-IR) spectroscopy. Furthermore, the antibacterial efficacy of the synthesized ZnO NPs against *X. oryzae* pv. *oryzae* was evaluated. Furthermore, the impact of the synthesized ZnO NPs on rice growth was examined by analyzing parameters such as plant height, root length, and photosynthetic pigments.

2. Materials and methods

2.1. Crude ethanol extract from mangosteen peel

Mangosteen peels were collected in May from residences in the district of Phayao, Phayao province, Northern Thailand. The collected samples underwent drying and grinding into powder. Subsequently, 2 g of the powder were extracted in 500 mL of 80 % ethanol for 30 min followed by cloth filtration. The resultant extract was then immediately used for biosynthesis of the ZnO NPs.

2.2. Green synthesis of ZnO NPs from ethanol extract of mangosteen peels

A 2 M solution of zinc acetate ($\text{Zn}(\text{CH}_3\text{COO})_2$) (Ajax Finechem, Australia) was prepared in deionized water by stirring for 20 min at room temperature. Then, 100 mL of crude extract at 4 mg/mL and 100 mL of the 2 M zinc acetate were separately introduced into burettes and added dropwise into a beaker at room temperature. The combined solution was continuously stirred for 1 h. Following this, 2 M NaOH (J.T. Baker, Malaysia) was incrementally added dropwise until a pH of 12 was achieved. The mixture underwent further agitation for 1 h and was then subjected to centrifugation for 30 min at $7880 \times g$ and 4°C (Biofuge Stratos, Sorvall, Germany). The obtained particles were subsequently dried at 80°C [5] until completely dry.

2.3. Identification of ZnO NPs using X-ray diffraction

CuK α radiation with a wavelength (λ) of 1.541 \AA , as described in Ref. [5], was employed for the analysis. The lattice parameters and crystallite sizes were determined based on Rietveld refinement using the MAUD software [22].

2.4. Analysis of ultraviolet–visible spectra

The UV–Vis spectra between 300 and 600 nm of the ZnO NPs dispersed in deionized water were analyzed using a UV-1800 spectrophotometer (SHIMADZU, Japan) in the photoluminescence mode. Then, the optical band gap of the particles was calculated using the Tauc plot method [23].

2.5. Scanning electron microscopy analysis

In accordance with the protocols described in Ref. [24]. The morphological characteristics of the synthesized ZnO NPs were investigated using a field emission scanning electron microscope (FEI, Quanta 450, OR, USA). Then, the particle sizes were averagely determined from 100 particles using the ImageJ software [25].

2.6. Analysis using Fourier transform infrared

The identification of functional group present in the synthesized ZnO NPs was conducted using an FT-IR spectrometer (Bruker, MA, USA). The biosynthesized ZnO NPs and the powder of mangosteen peel extract were scanned using the potassium bromide (KBr) method in the 400–4000 cm^{-1} infrared region with a 4 cm^{-1} resolution.

2.7. Antibacterial activity assay

The pure isolate of *X. oryzae* pv. *oryzae* (the pathogen causing rice bacterial blight), *Ralstonia solanacearum* (causing bacterial wilt) and *Xanthomonas axonopodis* pv. *citri* (associated with citrus canker) were obtained from the Plant Protection Research and Development Office, Bangkok, Thailand. *Staphylococcus aureus* (ATCC 29213) and methicillin-resistant *S. aureus* (MRSA) (ATCC BAA-1690) were purchased from The American Type Culture Collection (ATCC). Subsequently, all bacteria were cultured in Luria broth (1 % (w/v) peptone (HiMedia Laboratories Pvt.Ltd., India), 0.5 % (w/v) yeast extract (HiMedia Laboratories Pvt.Ltd., India) and 1 % (w/v) NaCl (JT Backer®, U.S.A.), maintained under constant shaking at 110 rpm at 37 °C (ES 20, Biosan, Latvia) until reaching an OD_{600} of 0.6. Following this, the antibacterial activity assay using ZnO NPs at concentration ranging from 0 to 10 mg/mL was conducted and analyzed as described in Ref. [18]. Moreover, the minimum inhibitory concentration (MIC) was also reported.

2.8. Plant materials and treatments

The *Oryza sativa* L. cv. KDML 105 rice seeds were sterilized by incubation at 60 °C for 3 days, followed by soaking for 1 day in deionized water to ensure uniformity of seedling growth. Then, all the rice seeds were placed on moist filter paper for 4 days to allow germination before transferring them to the pots. The plants were kept in a greenhouse with natural sunlight and watered once a day for 2 weeks. The treatments involved various concentrations of ZnO NPs (0, 0.95, 1.90, 3.80 mg/mL) being sprayed daily to the rice leaves for 7 days and the plant height, root length, and dry biomass were measured at the end of each experimental treatment.

2.9. Photosynthetic pigments analysis

The photosynthetic pigments of the rice plants aged 28 days were analyzed. Approximately 100 mg of the leaves were cut and immediately placed in liquid nitrogen. Then, the leaves were homogenized using a tissue homogenizer (Mixer mills 400, Retsch, Germany). The samples were incubated in 15 mL of 80 % (v/v) buffered acetone (80 mL of acetone mixed with 20 mL of 2.5 mM phosphate buffer, pH 7.8) at 4 °C for 24 h with continuous shaking [26]. Subsequently, the absorbance levels of chlorophyll a,

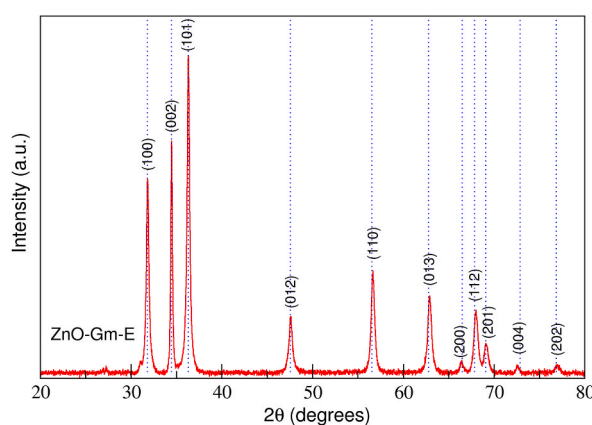


Fig. 1. XRD pattern of synthesized ZnO NPs from mangosteen ethanol extract.

chlorophyll b, total chlorophyll, and carotenoids were measured at 470, 645 and 663 nm using previously described equations [27,28].

2.10. Statistical evaluation

Differences among the samples were assessed for significance utilizing ANOVA and Tukey's multiple comparison test (GraphPad Software Prism9, San Diego, CA, USA). Statistical significance was considered at the $p < 0.05$ level.

3. Results and discussions

3.1. Characterization of synthesized ZnO NPs structure using XRD analysis

After incubation, the white powder weighing 17.83 g was obtained. The structures of the synthesized particles were analyzed using XRD with the hexagonal wurtzite index (JCPDS card No. 00036–1451) [29]. From Fig. 1, the XRD profiles confirmed the generation of wurtzite ZnO NPs without impurity. In addition, the appearance of sharp diffraction peaks with high signal-to-noise ratios suggested good crystallinity of the synthesized particles [30]. These synthesized ZnO NPs were designated as ZnO-Gm-E. The calculated average crystallite size was 387.122 Å (lattice parameter $a = 3.2540$ Å, $c = 5.2149$ Å). Thus, the crystallite size of ZnO-Gm-E was slightly bigger than that of the green synthesized ZnO NPs from mangosteen peel water extract (Crystallite size = 290.42 Å; lattice parameter $a = 3.2545$ Å, $c = 5.2126$ Å) reported by Jaithon et al. (2022). In contrast, effects of different solvents in synthesis of ZnO NPs using a chemical synthesis resulted in significant differences in size and morphology of the particles [20]. Taken all together, these combined results suggested that when the bioactive mangosteen peel compounds were presented in both strong and moderate polar solvents, they could serve as one or more of reducing, metal capping, or stabilizing agents. As a result, calcination is not required for the stable formation of biosynthesized ZnO NPs [31]. However, in several instances of biosynthesized ZnO NPs, calcination was performed to completely remove organic residues or other impurities from the surface of the particles [32]. It was found that longer calcination times increased the crystallite size of biosynthesized ZnO NPs [33].

3.2. UV-vis analysis of ZnO-Gm-E

Next, UV-Vis analysis was employed to determine the optical characteristics of the ZnO NPs. Other studies indicated that the λ_{\max} value of the ZnO NPs was in the range 300–400 nm [24,31,34]. In addition, the λ_{\max} values of ZnO NPs synthesized from water extract of mangosteen peel were reported as 365 nm [18] and 366 nm [35]. Likewise, the current study recorded a similar λ_{\max} value of 364 nm for ZnO-Gm-E (Fig. 2). Furthermore, the calculated average energy band gap was 2.88 eV, which is equivalent to that of spherical ZnO NPs synthesized from a water extract of mangosteen peel (2.79 eV). Davis et al. (2019) indicated that the optical band gaps of ZnO NPs generated using a sol-gel method with different solvent systems were in the range 3.10–3.37 eV [36]. On the other hand, ZnO NPs synthesized from chemical co-precipitation approaches were in the range 3.10–3.26 eV, depending on the morphology of the ZnO NPs [37]. Notably, most of the biosynthesized ZnO NPs were reported to have smaller band gaps (<3.00 eV) than from other methods [18, 38]. Given the narrower band gap, the prepared particles were classified as having strong photocatalytic activity because an electron could undergo excitation from the valence band to the conduction band. Several factors have been reported to affect the energy band gap, including oxygen deficiency, lattice strain, grain size, and surface roughness [39].

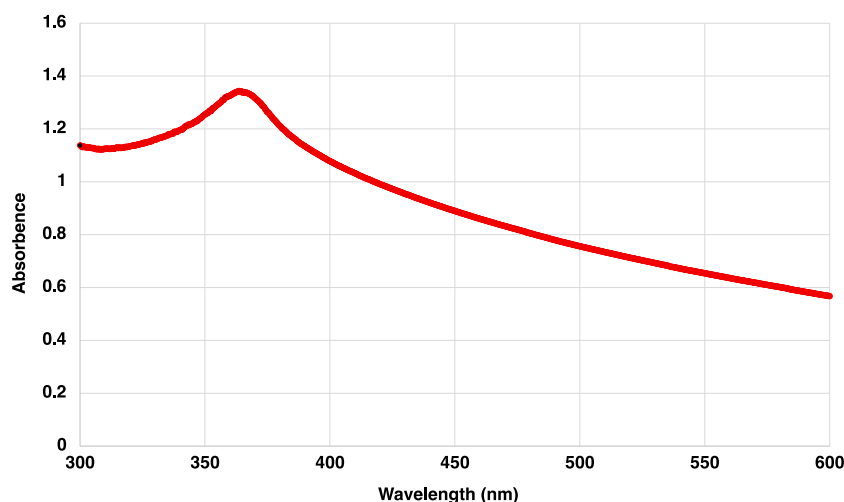


Fig. 2. UV-Vis spectrum of ZnO-Gm-E.

3.3. FTIR analysis of ZnO-Gm-E

From Fig. 3, the spectral peaks in the range 700–500 cm^{-1} of ZnO-Gm-E demonstrated the formation of the ZnO NPs. Furthermore, both the FTIR spectra of ZnO-Gm-E and mangosteen peel showed strong peaks in the region related to –OH vibration ($\sim 3500 \text{ cm}^{-1}$) and the stretching vibration of the carbonyl (C=O) around 1700–1400 cm^{-1} . These results supported other studies that found phytochemical constituents in extracts played important roles as the capping agents in the biosynthesis of nanoparticles [40,41].

3.4. Morphological characterization of ZnO-Gm-E using SEM analysis

The morphology of the nanoparticles significantly impacts their physicochemical characteristics [42]. From the SEM analysis, the ZnO-Gm-E particles almost had a spherical appearance (Fig. 4A) with an average size of $321 \pm 84 \text{ nm}$ (Fig. 4B). Despite utilizing different solvents for extracting mangosteen peels, this study produced ZnO-NPs of similar shapes but slightly bigger than the ZnO-Gm particles from mangosteen peel water extract (dimensions of $154.41 \times 172.89 \text{ nm}$) [18]. Some of the parameters in the synthetic conditions that have been shown to affect the particle morphology are plant extract concentration, reaction time, precursor concentration, and calcination temperature [43].

3.5. Antibacterial activity of ZnO-Gm-E against rice bacterial blight pathogen

X. oryzae pv. *oryzae* is responsible for a major rice disease known as rice bacterial blight disease in tropical Asian countries, as well as in Australia, Latin America, and Africa [44]. Infected rice species can undergo a minimum yield loss of 10 % and a maximum yield loss of 60 % during severe epidemics [45]. Although bactericides and antibacterial agents are frequently used to control the disease, they may be ineffective, have an adverse effect on non-target species, be harmful to the environment, or result in bactericide resistance [46]. Therefore, the ability of ZnO-Gm-E to inhibit the growth of *X. oryzae* pv. *oryzae* was evaluated. The results indicated that ZnO-Gm-E strongly inhibited viability against *X. oryzae* pv. *oryzae* with an IC_{50} value of 1.895 mg/mL and the MIC value at 4 mg/mL (Fig. 5). The results from other studies show that ZnO-Gm-E is markedly more potent than the isolated berberine from *Mahonia fortunei* ($\text{IC}_{50} = 2.9008 \text{ mg/mL}$) [47] and fruit extract from *Piper sarmentosum* ($\text{IC}_{50} = 24.69 \text{ mg/mL}$) [48]. In contrast, ZnO-Gm-E was weaker than the crude extract of *Alternaria alternata* ZHJG5 ($\text{IC}_{50} 29.5\text{--}74.1 \mu\text{M}$) and resveratrol ($\text{IC}_{50} 11.67 \pm 0.58 \mu\text{g/mL}$) [49]. Notably, the antibacterial activity of ZnO NPs has been reported to depend on the size and shape of the particles, which may relate to their specific mode of actions. Nevertheless, four main mechanisms of antibacterial activities have been proposed, including (i) the production of reactive oxygen species (ROS) [50], (ii) the loss of cellular integrity due to ZnO NPs contact [51], (iii) ZnO NPs internalization [52] and (iv) the release of Zn^{2+} ions in aqueous solution [53].

In addition, ZnO-Gm-E could also inhibit other plant pathogenic bacteria and human pathogenic bacteria (Table 1). Nevertheless, further experiment is required to evaluate the antibacterial activity of ZnO-Gm-E *in vivo*.

3.6. Effects of ZnO-GM-E on growth of rice plants

Several studies have reported the effects of nanoparticles on plant growth and secondary metabolite production [54,55]. Zinc, an indispensable element necessary for plant growth and development, has been extensively studied [56,57]. In the current study, different concentrations of ZnO-Gm-E were sprayed on the plants for 7 days to investigate its capability regarding plant growth promotion. No significant differences in plant height (Figs. 6a and 7a) were observed between the controls and plants treated with ZnO-Gm-E.

Nevertheless, at a concentration of 3.80 mg/mL, ZnO-Gm-E significantly enhanced both root length (Figs. 6b and 7c) and the dry biomass of the plants (Fig. 7b) in comparison to the deionized water treatment (control). These results suggested that ZnO-Gm-E did not negatively impact plant growth.

The chlorophyll content is widely accepted as a good indicator of photosynthetic capacity and hence plant growth. In the current study, the accumulation of chlorophylls and carotenoids was investigated (Fig. 8). The results showed that ZnO-Gm-E application (at 1.90 and 3.80 mg/mL) significantly ($p < 0.05$) increased the content of chlorophyll *a* (Fig. 8a), which is the major photosynthetic pigment. A similar result was found in olive trees [58]. The observed effects could be attributed to the potential influence of ZnO NPs

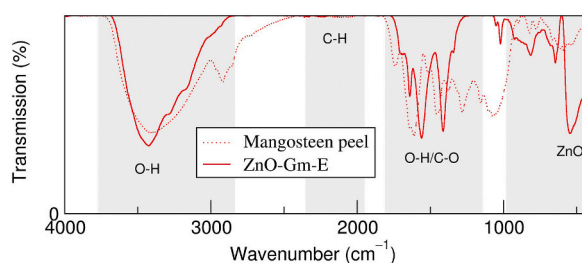


Fig. 3. FTIR analysis of ZnO-Gm-E and mangosteen peel.

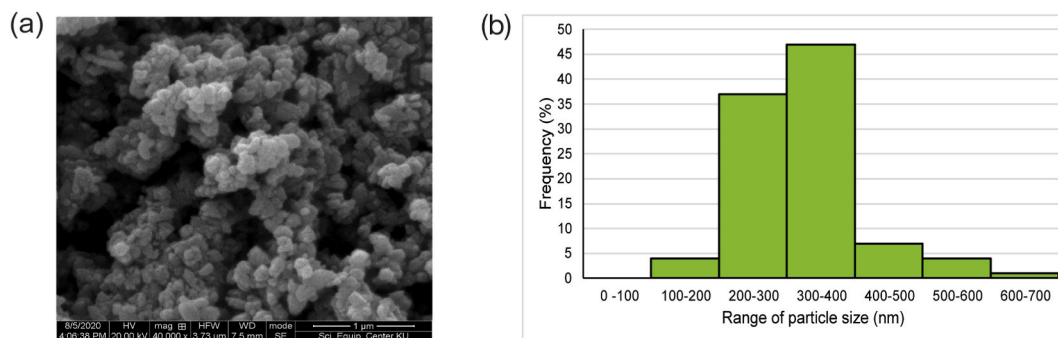


Fig. 4. SEM analysis ZnO-Gm-E morphology (a) Morphology (b) Frequency of particle size.

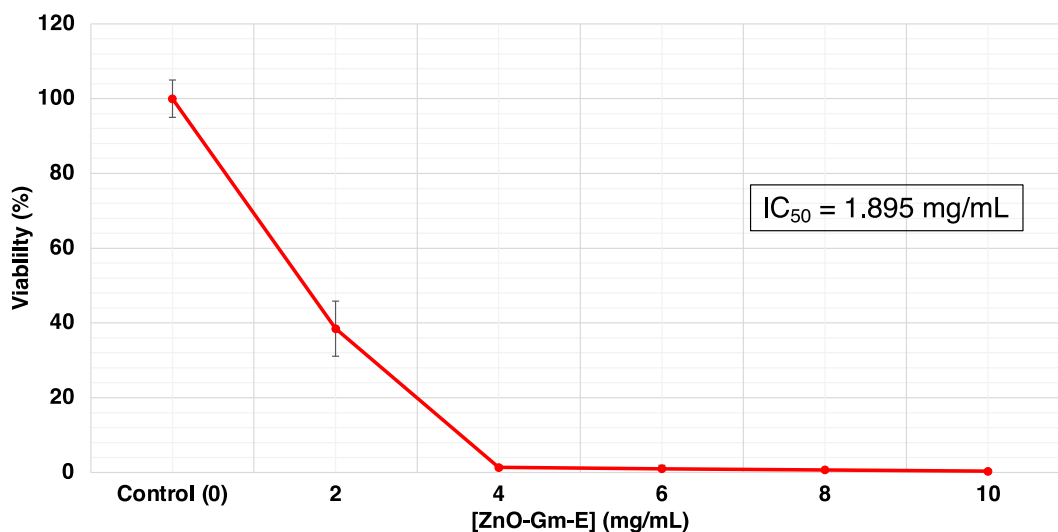


Fig. 5. Effect of ZnO Gm-E against viability of *X. oryzae* pv. *oryzae*. The IC_{50} was calculated and indicated. The data are represented in quadruplicates of mean \pm the standard error of mean from at least three independent experiments.

Table 1

The IC_{50} values of the ZnO-Gm-E against other pathogenic bacteria from this study.

Pathogenic bacteria	Disease	IC_{50} of ZnO-GM-E (mg/mL)
Plant pathogenic bacteria		
<i>Ralstonia solanacearum</i>	Bacterial wilt disease	2.091
<i>Xanthomonas axonopodis</i> pv. <i>citri</i>	Citrus canker	2.122
Human pathogenic bacteria		
<i>Staphylococcus aureus</i>	Skin and soft tissue infections	5.209
Methicillin-resistant <i>S. aureus</i> (MRSA)	Skin and soft tissue infections	5.430

on stimulating the gene expression of enzymes involved in chlorophyll biosynthesis [59]. Previous studies also demonstrated that NPs can elevate the photosynthetic rate by expediting water photolysis and the electron transport chain [60]. Altogether, these findings highlight the potential of ZnO-Gm-E as a fertilizer to promote rice growth.

ZnO NPs not only have the impact on plant growth under normal conditions, but they are also involved in plant stress tolerance mechanisms. Under chilling stress, supplementation with ZnO NPs positively impacted the plant height, root length, and dry biomass of rice plants compared to the controls [61]. Additionally, recent studies demonstrated that ZnO NPs are involved in drought [62] and arsenic stress tolerance [63]. Further studies are required to gain insight into the role of green synthesized ZnO-Gm-E on the stress tolerance mechanisms in rice and other plant species.

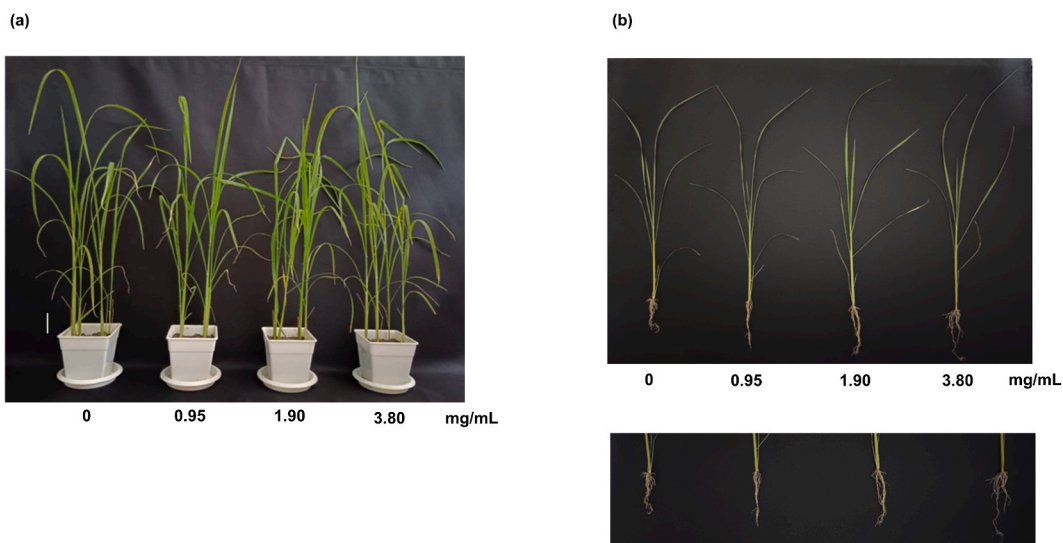


Fig. 6. Effect of different concentrations of ZnO-Gm-E on rice growth at 28 days post treatment. (a) plant height and (b) root length.

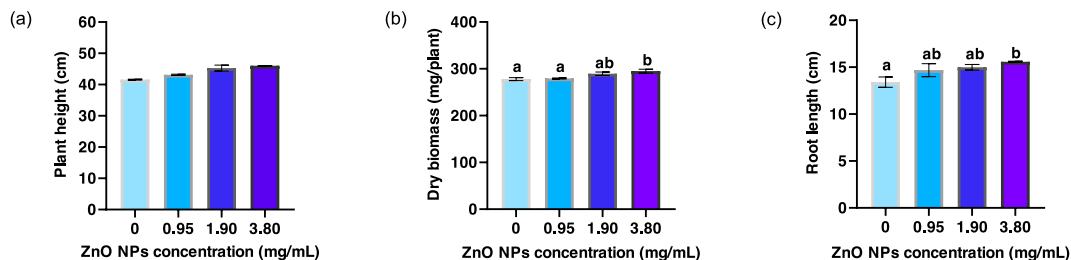


Fig. 7. Effect of different concentrations of ZnO-Gm-E on rice growth. Parameters recorded were: (a) plant height, (b) root length and (c) dry biomass. The data are the averages of 10 replicates, with the standard error of mean shown by the error bars. Different letters above error bars show differences at $p < 0.05$.

4. Conclusions

The current study was the first to demonstrate that the bioactive compounds found in mangosteen peel ethanol extract function as capping, reducing, and/or stabilizing agents in the biosynthesis of ZnO NPs with zinc acetate. The synthesized ZnO NPs, designated ZnO-Gm-E, had a spherical shape and a crystallite size of 38.71 nm (or 387.122 Å), with an average energy band gap of 2.88 eV. The λ_{\max} value of ZnO-Gm-E was at 364 nm. Based on the antibacterial activity assay, ZnO-Gm-E strongly inhibited the growth of rice bacterial leaf blight *in vitro* with an IC_{50} value of 1.895 mg/mL and the MIC value at 4 mg/mL. Additionally, at twofold IC_{50} (\sim MIC value), there was no toxicity regarding rice plant growth while there was a significant increase in photosynthetic pigment, chlorophyll *a*. Consequently, the results supported the potential use of fruit waste for the biosynthesis of ZnO NPs that could be utilized to supplement rice plants and to reduce infected rice disease due to bacteria.

Data availability

Data is not available to access in a data repository; however, it will be made available by the corresponding author upon request.

CRedit authorship contribution statement

Titiradsakorn Jaithon: Writing – original draft, Validation, Methodology, Investigation. **Thamonwan Atichakaro:** Writing – original draft, Methodology, Investigation, Funding acquisition. **Wannarat Phonphoem:** Writing – review & editing, Writing – original draft, Visualization, Validation, Supervision, Resources, Formal analysis, Conceptualization. **Jiraroj T-Thienprasert:** Writing – review & editing, Writing – original draft, Visualization, Supervision, Software, Data curation. **Tanee Sreewongchai:** Supervision. **Nattanan Panjaworayan T-Thienprasert:** Writing – review & editing, Writing – original draft, Visualization, Validation, Supervision, Resources, Project administration, Investigation, Funding acquisition, Formal analysis, Conceptualization.

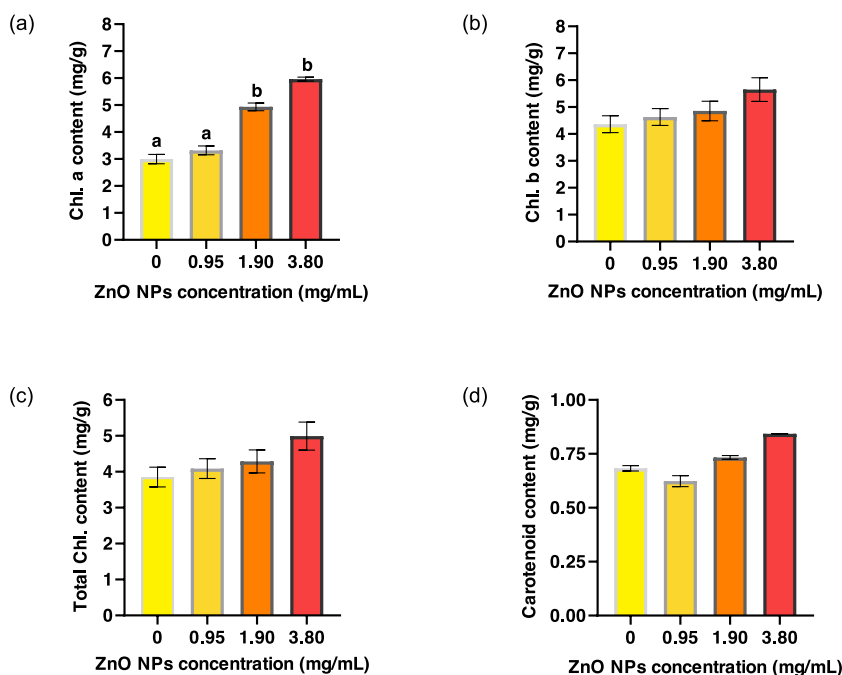


Fig. 8. Accumulation of photosynthetic pigments following ZnO-Gm-E treatments. (a) chlorophyll a, (b) chlorophyll b, (c) total chlorophylls and (d) carotenoids.

Declaration of competing interest

The authors declare that they have no known competing financial interests or personal relationships that could have appeared to influence the work reported in this paper.

Acknowledgement

This research is funded by Kasetsart University, Bangkok, Thailand through the Graduate School Fellowship Program. The article publishing charge has been supported by International SciKU Branding (ISB), Faculty of Science, Kasetsart University, Thailand. A sincere thank you to Dr Andrew Warner (Kasetsart University Research and Development Institute) for his diligent proofreading of this paper.

References

- [1] S. Raha, M. Ahmaruzzaman, ZnO nanostructured materials and their potential applications: progress, challenges and perspectives, *Nanoscale Adv.* 4 (8) (2022) 1868–1925.
- [2] S. Sabir, M. Arshad, S.K. Chaudhari, Zinc oxide nanoparticles for revolutionizing agriculture: synthesis and applications, *Sci. World J.* 2014 (2014) 925494.
- [3] M. Faizan, F. Yu, C. Chen, A. Faraz, S. Hayat, Zinc oxide nanoparticles help to enhance plant growth and alleviate abiotic stress: a review, *Curr. Protein Pept. Sci.* 22 (5) (2021) 362–365.
- [4] V.P. Aswathi, S. Meera, C.G.A. Maria, M. Nidhin, Green synthesis of nanoparticles from biodegradable waste extracts and their applications: a critical review, *Nanotechnol. Environ. Eng.* 8 (2023) 377–397.
- [5] J. Ruangtong, J. T-Thienprasert, N.P. T-Thienprasert, Green synthesized ZnO nanosheets from banana peel extract possess anti-bacterial activity and anti-cancer activity, *Mater. Today Commun.* 24 (2020) 101224.
- [6] S. Lopes, C.V. Borges, S.M. de Sousa Cardoso, M.F. de Almeida Pereira da Rocha, M. Maraschin, Banana (*musa spp.*) as a source of bioactive compounds for health promotion, *Handbook of Banana Production, Postharvest Science, Processing Technology, and Nutrition* (2020) 227–244.
- [7] S. Smaoui, H.B. Hlima, A.C. Mtibaa, M. Fourati, I. Sellem, K. Elhadef, et al., Pomegranate peel as phenolic compounds source: advanced analytical strategies and practical use in meat products, *Meat Sci.* 158 (2019) 107914.
- [8] O.J. Nava, C.A. Soto-Robles, C.M. Gómez-Gutiérrez, A.R. Vilchis-Nestor, A. Castro-Beltrán, A. Olivas, et al., Fruit peel extract mediated green synthesis of zinc oxide nanoparticles, *J. Mol. Struct.* 1147 (2017) 1–6.
- [9] R. Zadernowski, S. Czaplicki, M. Naczki, Phenolic acid profiles of mangosteen fruits (*Garcinia mangostana*), *Food Chem.* 112 (3) (2009) 685–689.
- [10] W. Pothitirat, R. Chomnawang Mt Fau - Supabphol, W. Supabphol R Fau - Gritsanapan, W. Gritsanapan, Comparison of bioactive compounds content, free radical scavenging and anti-acne inducing bacteria activities of extracts from the mangosteen fruit rind at two stages of maturity, *Fitoterapia* 80 (2009) 442–447.
- [11] J. Pedraza-Chaverri, N. Cárdenas-Rodríguez, M. Orozco-Ibarra, J.M. Pérez-Rojas, Medicinal properties of mangosteen (*Garcinia mangostana*), *Food Chem. Toxicol.* 46 (10) (2008) 3227–3239.
- [12] E.-Y. Ahn, S.-W. Shin, K. Kim, Y. Park, Facile green synthesis of titanium dioxide nanoparticles by upcycling mangosteen (*Garcinia mangostana*) pericarp extract, *Nanoscale Res. Lett.* 17 (1) (2022) 1–12.
- [13] J.S. Park, E.-Y. Ahn, Y. Park, Asymmetric dumbbell-shaped silver nanoparticles and spherical gold nanoparticles green-synthesized by mangosteen (*Garcinia mangostana*) pericarp waste extracts, *Int. J. Nanomed.* 12 (2017) 6895.

- [14] Y.-W. He, Je Wu, J.-S. Cha, L.-H. Zhang, Rice bacterial blight pathogen *Xanthomonas oryzae* pv. *oryzae* produces multiple DSF-family signals in regulation of virulence factor production, *BMC Microbiol.* 10 (1) (2010) 187.
- [15] Y. Xu, Q-q Luo, M-g Zhou, Identification and characterization of integron-mediated antibiotic resistance in the phytopathogen *Xanthomonas oryzae* pv. *oryzae*, *PLoS One* 8 (2) (2013) e55962.
- [16] Y. Gao, D. Xu, D. Ren, K. Zeng, X. Wu, Green synthesis of zinc oxide nanoparticles using *Citrus sinensis* peel extract and application to strawberry preservation: a comparison study, *LWT* 126 (2020) 109297.
- [17] C.A. Garza-Alonso, A. Juárez-Maldonado, S. González-Morales, M. Cabrera-De la Fuente, G. Cadenas-Pliego, A.B. Morales-Díaz, et al., ZnO nanoparticles as potential fertilizer and biostimulant for lettuce, *Heliyon* 9 (1) (2023) e12787.
- [18] T. Jaithon, J. Ruangtong, J. T-Thienprasert, N.P. T-Thienprasert, Effects of waste-derived ZnO nanoparticles against growth of plant pathogenic bacteria and epidermoid carcinoma cells, *Crystals* [Internet] 12 (6) (2022).
- [19] W. Suttirak, S. Manurakchinakorn, In vitro antioxidant properties of mangosteen peel extract, *J. Food Sci. Technol.* 51 (12) (2014) 3546–3558.
- [20] K.G. Kanade, B.B. Kale, R.C. Aiyer, B.K. Das, Effect of solvents on the synthesis of nano-size zinc oxide and its properties, *Mater. Res. Bull.* 41 (3) (2006) 590–600.
- [21] P.B. Khoza, M.J. Moloto, L.M. Sikhwivhili, The effect of solvents, acetone, water, and ethanol, on the morphological and optical properties of ZnO nanoparticles prepared by microwave, *Journal of Nanotechnology* 2012 (2012) 195106.
- [22] L. Lutterotti, Total pattern fitting for the combined size–strain–stress–texture determination in thin film diffraction, *Nucl. Instrum. Methods Phys. Res. Sect. B Beam Interact. Mater. Atoms* 268 (3–4) (2010) 334–340.
- [23] J. Tauc, Optical properties and electronic structure of amorphous Ge and Si, *Mater. Res. Bull.* 3 (1) (1968) 37–46.
- [24] N.P. T-Thienprasert, J. T-Thienprasert, J. Ruangtong, T. Jaithon, P. Srifah Huehne, O. Piasai, Large scale synthesis of green synthesized zinc oxide nanoparticles from banana peel extracts and their inhibitory effects against *colletotrichum* sp., isolate KUFC 021, causal agent of anthracnose on *dendrobium* orchid, *J. Nanomater.* 2021 (2021) 5625199.
- [25] C.T. Rueden, J. Schindelin, M.C. Hiner, B.E. DeZonia, A.E. Walter, E.T. Arena, et al., ImageJ2: ImageJ for the next generation of scientific image data, *BMC Bioinf.* 18 (1) (2017) 1–26.
- [26] P. Krishnan, I. Ravi, S.K. Nayak, Methods for estimating the chlorophyll content in rice leaves: a reappraisal, *Indian J. Exp. Biol.* 34 (1996) 1030–1033.
- [27] Y. Aono, Y. Asikin, N. Wang, D. Tieman, H. Klee, M. Kusano, High-throughput chlorophyll and carotenoid profiling reveals positive associations with sugar and apocarotenoid volatile content in fruits of tomato varieties in modern and wild accessions, *Metabolites* [Internet] 11 (6) (2021).
- [28] D.I. Arnon, Copper enzymes in isolated chloroplasts. Polyphenoloxidase in *beta vulgaris*, *Plant Physiol* 24 (1) (1949) 1–15.
- [29] R. Jenkins, T.G. Fawcett, D.K. Smith, J.W. Visser, M.C. Morris, L.K. Frevel, JCPDS—international centre for diffraction data sample preparation methods in X-Ray Powder Diffraction, *Powder Diffraction* 1 (2) (1986) 51–63.
- [30] C.F. Holder, R.E. Schaak, Tutorial on powder X-ray diffraction for characterizing nanoscale materials, *ACS Nano* 13 (7) (2019) 7359–7365.
- [31] D. Jevapatarakul, J. T-Thienprasert, S. Payungporn, T. Chavalit, A. Khamwut, N.P. T-Thienprasert, Utilization of *Cratogeomys formosus* crude extract for synthesis of ZnO nanosheets: characterization, biological activities and effects on gene expression of nonmelanoma skin cancer cell, *Biomed. Pharmacother.* 130 (2020) 110552.
- [32] S. Zeghoud, H. Hemmami, B. Ben Seghir, I. Ben Amor, I. Kouadri, A. Rebiai, et al., A review on biogenic green synthesis of ZnO nanoparticles by plant biomass and their applications, *Mater. Today Commun.* 33 (2022) 104747.
- [33] M.H. Koupaei, B. Shareghi, A.A. Saboury, F. Davar, A. Semnani, M. Evini, Green synthesis of zinc oxide nanoparticles and their effect on the stability and activity of proteinase K, *RSC Adv.* 6 (48) (2016) 42313–42323.
- [34] Z. Song, T.A. Fau - Kelf, W.H. Kelf Ta Fau - Sanchez, M.S. Sanchez Wh Fau - Roberts, J. Roberts Ms Fau - Rička, M. Rička J Fau - Frenz, M. Frenz, A.V. Fau - Zvyagin, et al., Characterization of optical properties of ZnO nanoparticles for quantitative imaging of transdermal transport, *Biomed. Opt Express* 2 (12) (2011) 3321–3333.
- [35] K.A.S.S. Kuruppu, K.M.K.G. Perera, A.M.R. Chamara, G. Thiripuranathar, Flower shaped ZnO—NPs; phytofabrication, photocatalytic, fluorescence quenching, and photoluminescence activities, *Nano Express* 1 (2) (2020) 020020.
- [36] K. Davis, R. Yarbrough, M. Froeschle, J. White, H. Rathnayake, Band gap engineered zinc oxide nanostructures via a sol–gel synthesis of solvent driven shape-controlled crystal growth, *RSC Adv.* 9 (26) (2019) 14638–14648.
- [37] S. Agarwal, L. Jangir, K.S. Rathore, M. Kumar, K. Awasthi, Morphology-dependent structural and optical properties of ZnO nanostructures, *Appl. Phys. A* 125 (2019).
- [38] S. Faisal, H. Jan, S.A. Shah, S. Shah, A. Khan, M.T. Akbar, et al., Green synthesis of zinc oxide (ZnO) nanoparticles using aqueous fruit extracts of myristica fragrans: their characterizations and biological and environmental applications, *ACS Omega* 6 (14) (2021) 9709–9722.
- [39] F.-H. Wang, C.-L. Chang, Effect of substrate temperature on transparent conducting Al and F co-doped ZnO thin films prepared by rf magnetron sputtering, *Appl. Surf. Sci.* 370 (2016) 83–91.
- [40] N. Mude, A. Ingle, A. Gade, M. Rai, Synthesis of silver nanoparticles using callus extract of carica papaya — a first report, *J. Plant Biochem. Biotechnol.* 18 (1) (2009) 83–86.
- [41] J. Singh, T. Dutta, K.-H. Kim, M. Rawat, P. Samddar, P. Kumar, 'Green' synthesis of metals and their oxide nanoparticles: applications for environmental remediation, *J. Nanobiotechnol.* 16 (1) (2018) 84.
- [42] N. Babayevska, Przysiecka Ł, I. Iatsunskyi, G. Nowaczyk, M. Jarek, E. Janiszewska, et al., ZnO size and shape effect on antibacterial activity and cytotoxicity profile, *Sci. Rep.* 12 (1) (2022) 8148.
- [43] J. Xu, Y. Huang, S. Zhu, N. Abbes, X. Jing, L. Zhang, A review of the green synthesis of ZnO nanoparticles using plant extracts and their prospects for application in antibacterial textiles, *Journal of Engineered Fibers and Fabrics* 16 (2021) 155892502110462.
- [44] J.W.Y.F. Chan, P.H. Goodwin, The molecular genetics of virulence of *Xanthomonas campestris*, *Biotechnol. Adv.* 17 (6) (1999) 489–508.
- [45] N.V.L. Rajarajeswari, K. Muralidharan, Assessments of farm yield and district production loss from bacterial leaf blight epidemics in rice, *Crop Protect.* 25 (3) (2006) 244–252.
- [46] Y. Tian, Y. Zhao, R. Xu, F. Liu, B. Hu, R.R. Walcott, Simultaneous detection of *Xanthomonas oryzae* pv. *oryzae* and *X. oryzae* pv. *oryzicola* in rice seed using a padlock probe-based assay, *Phytopathology* 104 (10) (2014) 1130–1137.
- [47] G. Yuan, Y. Chen, F. Li, R. Zhou, Q. Li, W. Lin, et al., Isolation of an antibacterial substance from *Mahonia fortunei* and its biological activity against *Xanthomonas oryzae* pv. *oryzicola*, *J. Phytopathol.* 165 (5) (2017) 289–296.
- [48] S.F. Syed Ab Rahman, K. Sijam, D. Omar, Chemical composition of *Piper sarmentosum* extracts and antibacterial activity against the plant pathogenic bacteria *Pseudomonas fuscovaginae* and *Xanthomonas oryzae* pv. *oryzae*, *J. Plant Dis. Prot.* 121 (6) (2014) 237–242.
- [49] S. Zhao, C. Xiao, J. Wang, K. Tian, W. Ji, T. Yang, et al., Discovery of natural FabH inhibitors using an immobilized enzyme column and their antibacterial activity against *Xanthomonas oryzae* pv. *oryzae*, *J. Agric. Food Chem.* 68 (48) (2020) 14204–14211.
- [50] K.R. Raghupathi, R.T. Koodali, A.C. Manna, Size-Dependent bacterial growth inhibition and mechanism of antibacterial activity of zinc oxide nanoparticles, *Langmuir* 27 (7) (2011) 4020–4028.
- [51] L. Zhang, Y. Jiang, Y. Ding, M. Povey, D. York, Investigation into the antibacterial behaviour of suspensions of ZnO nanoparticles (ZnO nanofluids), *J. Nanoparticle Res.* 9 (3) (2007) 479–489.
- [52] R. Brayner, R. Ferrarilli, N. Brivois, S. Djediat, M.F. Benedetti, F. Fiévet, Toxicological impact studies based on *Escherichia coli* bacteria in ultrafine ZnO nanoparticles colloidal medium, *Nano Lett.* 6 (4) (2006) 866–870.
- [53] M. Li, L. Zhu, D. Lin, Toxicity of ZnO nanoparticles to *Escherichia coli*: mechanism and the influence of medium components, *Environ. Sci. Technol.* 45 (5) (2011) 1977–1983.
- [54] G. Marslin, C.J. Sheeba, G. Franklin, Nanoparticles alter secondary metabolism in plants via ROS burst, *Front. Plant Sci.* 8 (2017).

- [55] A. Rastogi, M. Zivcak, O. Sytar, H.M. Kalaji, X. He, S. Mbarki, et al., Impact of metal and metal oxide nanoparticles on plant: a critical review, *Front. Chem.* 5 (2017).
- [56] G. Hacisalihoglu, Zinc (Zn): the last nutrient in the alphabet and shedding light on Zn efficiency for the future of crop production under suboptimal Zn, *Plants [Internet]* 9 (11) (2020).
- [57] A. Sharma, B. Patni, D. Shankhdhar, S.C. Shankhdhar, Zinc – an indispensable micronutrient, *Physiol. Mol. Biol. Plants* 19 (1) (2013) 11–20.
- [58] L. Regni, D. Del Buono, M. Micheli, S.L. Facchin, C. Tolisano, P. Proietti, Effects of biogenic ZnO nanoparticles on growth, physiological, biochemical traits and antioxidants on olive tree in vitro, *Horticulturae [Internet]* 8 (2) (2022).
- [59] C. Chen, J. Lai, H. Chen, F. Yu, Zinc oxide nanoparticles enhanced growth of tea trees via modulating antioxidant activity and secondary metabolites, *Horticulturae [Internet]* 9 (6) (2023).
- [60] S. Pradhan, P. Patra, S. Das, S. Chandra, S. Mitra, K.K. Dey, et al., Photochemical modulation of biosafe manganese nanoparticles on vigna radiata: a detailed molecular, biochemical, and biophysical study, *Environ. Sci. Technol.* 47 (22) (2013) 13122–13131.
- [61] Y. Song, M. Jiang, H. Zhang, R. Li, Zinc oxide nanoparticles alleviate chilling stress in rice (*Oryza sativa* L.) by regulating antioxidative system and chilling response transcription factors, *Molecules* 26 (8) (2021).
- [62] L. Sun, F. Song, X. Zhu, S. Liu, F. Liu, Y. Wang, et al., Nano-ZnO alleviates drought stress via modulating the plant water use and carbohydrate metabolism in maize, *Arch. Agron Soil Sci.* 67 (2) (2021) 245–259.
- [63] S. Yan, F. Wu, S. Zhou, J. Yang, X. Tang, W. Ye, Zinc oxide nanoparticles alleviate the arsenic toxicity and decrease the accumulation of arsenic in rice (*Oryza sativa* L.), *BMC Plant Biol.* 21 (1) (2021) 150.